Methylruthenium Carbidocarbonyl Clusters supported on Inorganic Oxides: Characterization and Selective Acetaldehyde Formation

Yasuo Izumi,[a] Tai-Hui Liu,[a] Kiyotaka Asakura,[a] Teiji Chihara,[b] Hiroshi Yamazaki[b] and Yasuhiro Iwasawa*[,a]

[a] *Department of Chemistry, Faculty of Science, The University of Tokyo, Hongo, Bunkyo-ku, Tokyo 113, Japan*

[b] *The Institute of Physical and Chemical Research, Wako-shi, Saitama 351-01, Japan*

The clusters $[Ru_6C(CO)_{16}Me]^-$ supported on SiO_2, Al_2O_3 and TiO_2 were characterized by means of extended X-ray absorption fine structure (EXAFS), temperature-programmed desorption (TPD) and Fourier-transform IR spectroscopy in relation to developments of new catalytic systems. The EXAFS analysis revealed that the Ru_6C cluster framework which has an interstitial carbon atom was stable at 473 (SiO_2), 523 (Al_2O_3) and 473 K (TiO_2) under CO or CO + H_2. The supported clusters produced methane upon heating in vacuum by the reaction with surface hydrogen-bonded OH groups, whereas in the presence of CO + H_2 acetaldehyde was preferably produced, unlike $[Ru_6C(CO)_{16}Me]^-$ in a homogeneous system where only methane was formed. The selectivity to acetaldehyde was larger with SiO_2 (77%) than with Al_2O_3 (15) or TiO_2 (10%).

Insertion of CO into the co-ordination sphere of metal atoms has been extensively studied from chemical as well as industrial points of view. Most of the insertion steps are believed to proceed by alkyl migration according to experimental[1-3] and theoretical[4-6] work.

Insertion of CO is also a key elementary step associated with catalytic alkene hydroformylation, hydrogenation of CO, *etc.* For ethene hydroformylation on anion-doped rhodium catalysts,[7,8] the acyl intermediate (C_2H_5CO) is formed by insertion of CO into ethyl as suggested by IR spectra. While alkene hydroformylation proceeds on mononuclear metal complexes in homogeneous systems, metal clusters/particles are more active than highly dispersed/isolated metal sites in supported metal systems. In this context it is of interest to examine the reaction of ligands on a metal cluster framework supported on inorganic oxides. However, cluster frameworks are often decomposed to ill defined particles under catalytic reaction conditions.

In the present study a ruthenium carbidocarbonyl cluster $[Ru_6C(CO)_{16}Me]^-$ was supported on oxide surfaces. This compound with a methyl and carbonyl ligands has been reported to be converted into $[Ru_6C(CO)_{16}(COMe)]^-$ in a homogeneous system,[9] but its hydrogenation with H_2 did not proceed, resulting instead in decomposition to methane *via* a reverse reaction.[10] We report the characterization of $[Ru_6C(CO)_{16}Me]^-$ supported on SiO_2, Al_2O_3 and TiO_2 under various conditions by means of temperature-programmed desorption (TPD), extended X-ray absorption fine structure (EXAFS) and Fourier transform IR spectroscopy, and the formation of acetaldehyde from the supported cluster and hydrogen. Another aim of the study is to develop a new catalytic system for hydroformylation by controlling the chemical properties of the Ru_6 framework using an interstitial carbon as a four-electron donor. The supported cluster showed a high selectivity for catalytic ethene hydroformylation as compared with usual impregnated ruthenium catalysts, which will be reported in a separate paper.

Experimental

Preparation of Supported Ruthenium Clusters.—The compound $[NMe_3(CH_2Ph)][Ru_6C(CO)_{16}Me]$ **1** was synthesized in a similar way to that of $[N(PPh_3)_2][Ru_6C(CO)_{16}Me]$.[9] The framework of $[Ru_6C(CO)_{16}Me]^-$ is shown in Fig. 1. Silica (Fuji-Davison, silica gel no. 952; surface area 300 m^2 g^{-1}), Al_2O_3 (Degussa Alon C; surface are 100 m^2 g^{-1}) and TiO_2 (Degussa P25, surface area 50 m^2 g^{-1}) were heated at 473 K in a vacuum before use as supports for the ruthenium cluster. The treated oxides were impregnated with a methanol solution of **1**, followed by evaporation of the solvent. The loadings of **1** were 3.0% (w/w) Ru for SiO_2, 1.5% for Al_2O_3 and 5.0% for TiO_2 for the convenience of EXAFS experiments. These procedures were conducted at room temperature in a high-purity argon atmosphere (99.9999%) to avoid contacting with the air.

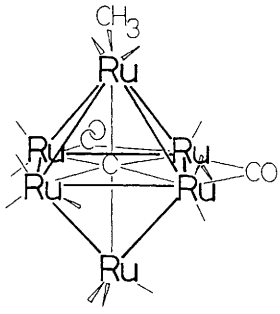

Fig. 1 The crystal structure of $[Ru_6C(CO)_{16}Me]^-$[9]

TPD Measurements.—TPD spectra were measured in a closed circulating system equipped with a gas chromatograph (heating rate 4 K min^{-1}). Methane and CO were analysed on 5A molecular sieve (2 m) at 353 K, and acetaldehyde, formaldehyde, dimethyl ether and methanol were analysed by dioctyl sebacate (4 m) at 353 K. Other hydrocarbons such as ethane and ethene were analysed on VZ-10 (GL Science Co.) (2 m).

EXAFS Spectra.—Ru K-edge EXAFS spectra were measured at room temperature at beamline 10B of the Photon Factory in

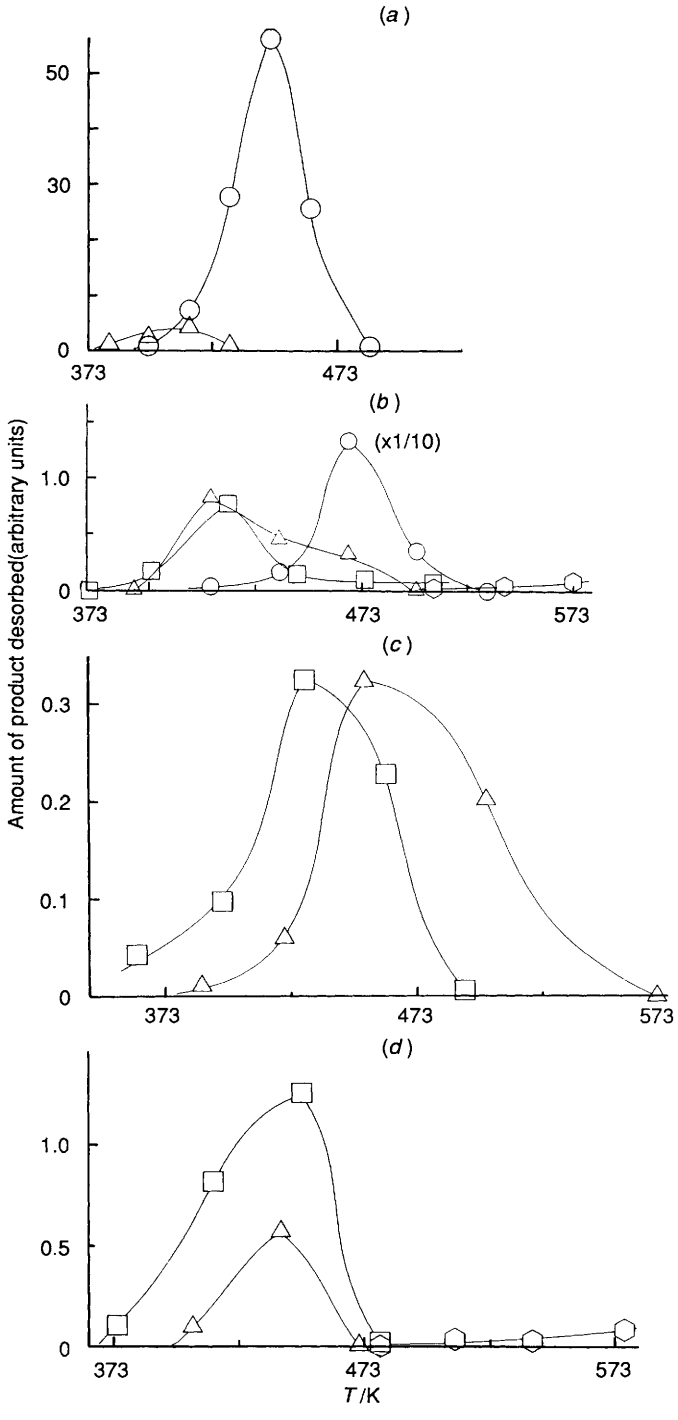

Fig. 2 The TPD spectra for $[Ru_6C(CO)_{16}Me]^-$–SiO_2: (*a*) under vacuum; (*b*) under H_2 (16.0 kPa); (*c*) under CO (16.0 kPa); (*d*) under CO (16.0 kPa) and H_2 (3.3 kPa). Heating rate 4 K min^{-1}. Products: CO (○), CH_4 (△), MeCHO (□) and MeOH (⬡)

the National Laboratory for High Energy Physics. The EXAFS analysis was carried out by subtracting a smoothly varying part estimated from a cubic spline and normalizing the spectrum to the absorption edge height in a similar procedure to that described previously.[11] The curve-fitting analysis was performed by using the phase shifts and amplitude functions of model compounds {**1** itself for Ru–C(carbonyl) and Ru(–C–)Ru (Ru–Ru second co-ordination) bonds, $[\{RuCl_2(CO)_3\}_2]$ for Ru(–C–)O(carbonyl), and ruthenium foil for Ru–Ru bonds}. This use of **1** to provide empirical parameters for Ru(–C–)Ru may be a reasonable approximation as long as the structural unit does not change much. The second peak in Fourier transforms for supported clusters may include two shells of Ru–Ru and Ru(–C–)O bonds. To avoid the possibility of a local minimum in the two-shell curve-fitting procedure, we compared the results with those obtained by fitting with one shell of Ru–Ru or Ru(–C–)O. The contributions of the different types of CO groups to the Ru(–C–)O shell are described later. The co-ordination number (N) bond distance (d) and Debye–Waller factor (σ) were determined in the fitting procedure.

IR Spectra.—Silica (0.06 g) was pressed to a disk which was placed in an IR cell with two NaCl windows, equipped with a closed circulating system. This disk was heated at 473 K in the cell, and impregnated dropwise with a methanol solution of cluster **1** by using a glass capillary in an argon (99.9999%) atmosphere without contact with the air. The IR spectra for these samples were measured on a JASCO FTIR-7000 spectrometer.

Results

TPD Spectra.—TPD spectra reflect the chemical properties and the degree of chemical interaction of $[Ru_6C(CO)_{16}Me]^-$ with oxides (SiO_2, Al_2O_3 or TiO_2). Upon supporting no gas evolution was observed.

$[Ru_6C(CO)_{16}Me]^-$–SiO_2. Spectra were observed under four conditions (under vacuum, H_2, CO, and CO + H_2) as shown in Fig. 2(*a*)–2(*d*). Fig. 2(*a*) shows that the methyl ligand quantitatively reacted with surface OH groups of SiO_2 to form the corresponding amount of methane at 373–423 K. After this reaction CO began to desorb. Under 16 kPa H_2 [Fig. 2(*b*)], acetaldehyde was produced (43% of methyl ligand) around 410 K besides methane formation (57% of methyl ligand). The carbon monoxide desorption temperature shifted toward higher value as compared with Fig. 2(*a*) (under vacuum). In a homogeneous system, however, methane was formed and acetaldehyde was never detected.[10] The TPD spectrum under 16 kPa CO [Fig. 2(*c*)] shows the shift of two peaks to higher temperatures because of a stabilization of the supported cluster by gas-phase CO, as confirmed by EXAFS. Fig. 2(*d*) is the TPD spectrum taken under a mixture of CO (16 kPa) and H_2 (3.3 kPa), where a high selectivity for acetaldehyde formation (77%) was observed.

$[Ru_6C(CO)_{16}Me]^-$–Al_2O_3. The TPD spectra for $[Ru_6C(CO)_{16}Me]^-$–Al_2O_3 are shown under two conditions (under H_2 and CO + H_2) in Fig. 3(*a*) and 3(*b*). Under vacuum the methyl ligand reacted with surface OH groups of Al_2O_3 to form methane similarly to the case of SiO_2. The species $[Ru_6C(CO)_{16}]$ on Al_2O_3 is formed at *ca.* 470 K. In the presence of 16 kPa H_2 [Fig. 3(*a*)] acetaldehyde (8% of methyl ligand) was evolved around 433 K besides methane (92% of methyl ligand); 15.3 CO molecules per Ru cluster were desorbed. Methanol may be formed by the hydrogenation of CO ligands. The total carbon amounts desorbed corresponded to 17 C per one supported cluster.

The formation of methanol was also observed in CO (16 kPa) + H_2 (3.3 kPa) [Fig. 3(*b*)]. During heating of the supported clusters the acetaldehyde formed in the TPD under CO corresponded to only 3.0% of the methyl ligand, but under a mixture of CO and H_2 [Fig. 3(*b*)] the selectivity to acetaldehyde increased to 15%.

$[Ru_6C(CO)_{16}Me]^-$–TiO_2. The TPD spectrum for $[Ru_6C(CO)_{16}Me]^-$–TiO_2 under vacuum was taken similarly to the cases of SiO_2 and Al_2O_3. The temperature of methane formation from the methyl ligand and the surface OH groups of TiO_2 was similar to that in the case of SiO_2. Carbon monoxide desorbed at 423–583 K, showing a relatively broader peak. The spectrum under CO + H_2 (Fig. 4) showed a high methane selectivity (90%) from methyl ligand, while the formation of acetaldehyde was 10% of the methyl ligand.

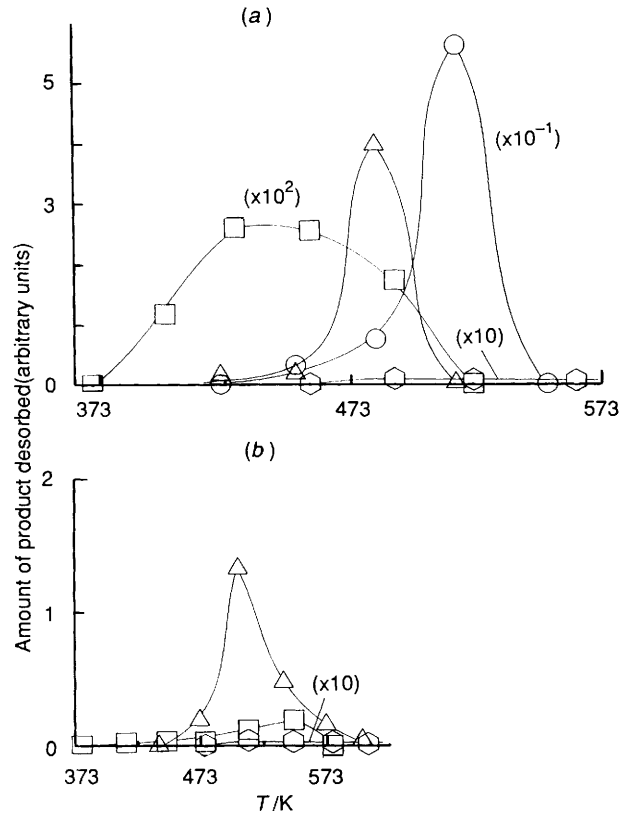

Fig. 3 The TPD spectra for $[Ru_6C(CO)_{16}Me]^-$–Al_2O_3: (*a*) under H_2 (16.0 kPa); (*b*) under CO (16.0 kPa) and H_2 (3.3 kPa); Heating rate and products as in Fig. 2

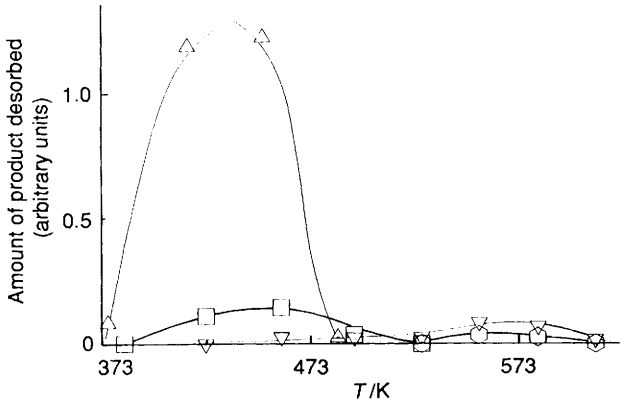

Fig. 4 The TPD spectrum for $[Ru_6C(CO)_{16}Me]^-$–TiO_2 under CO (16.0 kPa) and H_2 (3.3 kPa). Heating rate and products as in Fig. 2, except Me_2O (▽)

EXAFS Measurements.—$[Ru_6C(CO)_{16}Me]^-$–SiO_2. The EXAFS spectra of $[Ru_6C(CO)_{16}Me]^-$–SiO_2 were taken under various conditions. Fig. 5 shows the data for the incipient supported ruthenium cluster before treatment. Fig. 5(*a*) is the EXAFS oscillation and its associated Fourier transform is shown in Fig. 5(*b*) which has three peaks around 1.3, 2.3 and 3.7 Å (phase shift uncorrected). The peak lower than 1.0 Å remained irrelevantly to the spline region for the background subtraction by the cubic spline method in the analysing procedure, but fortunately this does not significantly affect the following discussion. By comparison with the EXAFS oscillation and its associated Fourier transform for $[NMe_3(CH_2Ph)][Ru_6C(CO)_{16}Me]$, the three peaks are assigned to Ru–C(carbonyl), Ru–Ru (first co-ordination) + Ru(–C–)O (carbonyl), and Ru(–C–)Ru (Ru–Ru second co-ordination) bonds, respectively. The curve-fitting results for these peaks are shown in Fig. 5(*c*)–5(*e*).

The best-fit results are shown in Table 1. The analysis of the second peak (1.95–3.15 Å) in the Fourier transform was first, conducted with one shell {Ru–Ru [Fig. 5(*d'*)] or Ru(–C–)O [Fig. 5(*d''*)]} in k = 4–12 Å^{-1}. However, this did not give good fits (R = 0.045 and 0.063, respectively as shown in Table 1). Next, we performed a two-shell [Ru–Ru + Ru(–C–)O] fitting which well reproduced the experimental curve in Fig. 5(*d*) (R = 0.025). The Ru(–C–)O shell is a composite of terminal, semi-bridging, and edge-bridging CO groups and hence the different Ru–C–O angles may modulate the phase and amplitude of these components. However, a three-shell [Ru–Ru + two Ru(–C–)O] fitting did not significantly improve the two-shell fit. It would not be valid to discriminate the different CO components in the present samples by EXAFS. The EXAFS data for Ru–Ru were not changed by the three-shell fitting.

Upon heating the incipient supported ruthenium cluster to 473 K under vacuum the EXAFS oscillation and Fourier transform [Fig. 6(*a*) and 6(*b*)] drastically changed to exhibit only one peak due to the Ru–Ru bonds. The Ru–Ru bond distance was determined to be 2.65 Å by the curve-fitting analysis (Table 1). The lack of Ru(–C–)Ru bonds suggests a change of Ru_6C structure at 473 K under vacuum. However, the co-ordination number of Ru–Ru bonds was 4.2 (Table 1), suggesting the retention of the Ru_6 unit on SiO_2.

In contrast to the instability of the clusters on SiO_2 at >423 K under vacuum, the structure of the ruthenium clusters on SiO_2 under CO (13.3 kPa) and H_2 (13.3 kPa) was retained until 473 K according to the EXAFS oscillation and Fourier transform in Fig. 7(*a*) and 7(*b*). The lengths and co-ordination numbers for the Ru–C, Ru–Ru, Ru(–C–)O and Ru(–C–)Ru bonds determined by the curve-fitting analysis in Fig. 7(*c*)–7(*e*) are listed in Table 2, and confirm the retention of the cluster framework at 473 K. The EXAFS data for the sample heated at 523 K under CO + H_2 showed only Ru–Ru bonds at 2.66 Å with a co-ordination number of 4.5 similar to that at 473 K in vacuum.

$[Ru_6C(CO)_{16}Me]^-$–Al_2O_3. The EXAFS data and the best-fit results for the incipient supported cluster $[Ru_6C(CO)_{16}Me]^-$–Al_2O_3 at 293 K are shown in Fig. 8 and Table 3. These results demonstrate that the cluster retained its original structure similarly to the case of the SiO_2 system. The co-ordination numbers of the Ru–C, Ru–Ru, Ru(–C–)O and Ru(–C–)Ru bonds drastically decreased at 473 K under vacuum. After heating the sample to 673 K under vacuum only one peak due to the Ru–Ru bonds was observed, similarly to the case of heated samples on SiO_2. The EXAFS oscillation suggested a metallic nature of Ru as in the case of the SiO_2 system [Fig. 6(*a*)], and the Ru–Ru bond distance was 2.63 Å according to the curve-fitting analysis.

Fig. 9 shows the EXAFS data for the Al_2O_3-supported cluster treated at 523 K under a mixture of CO (13.3 kPa) and H_2 (13.3 kPa). The oscillation and its associated Fourier transform resemble those of the incipient $[Ru_6C(CO)_{16}Me]^-$–Al_2O_3 in Fig. 8. The best-fit results are listed in Table 4, where data for the samples treated at 293, 373, 473 and 573 K under CO + H_2 are also shown. The EXAFS oscillation changed on heating at 573 K, where only a Fourier-transform peak due to the Ru–Ru bonds was observed. However, the corresponding co-ordination number was 4.2 similar to 3.9 for the incipient cluster.

$[Ru_6C(CO)_{16}Me]^-$–TiO_2. The EXAFS oscillation and its associated Fourier transform for $[Ru_6C(CO)_{16}Me]^-$–TiO_2 treated at 473 K under CO (13.3 kPa) + H_2 (13.3 kPa) suggest the similarity of the structures of supported and unsupported carbido clusters. The curve-fitting analysis in Table 5 confirms

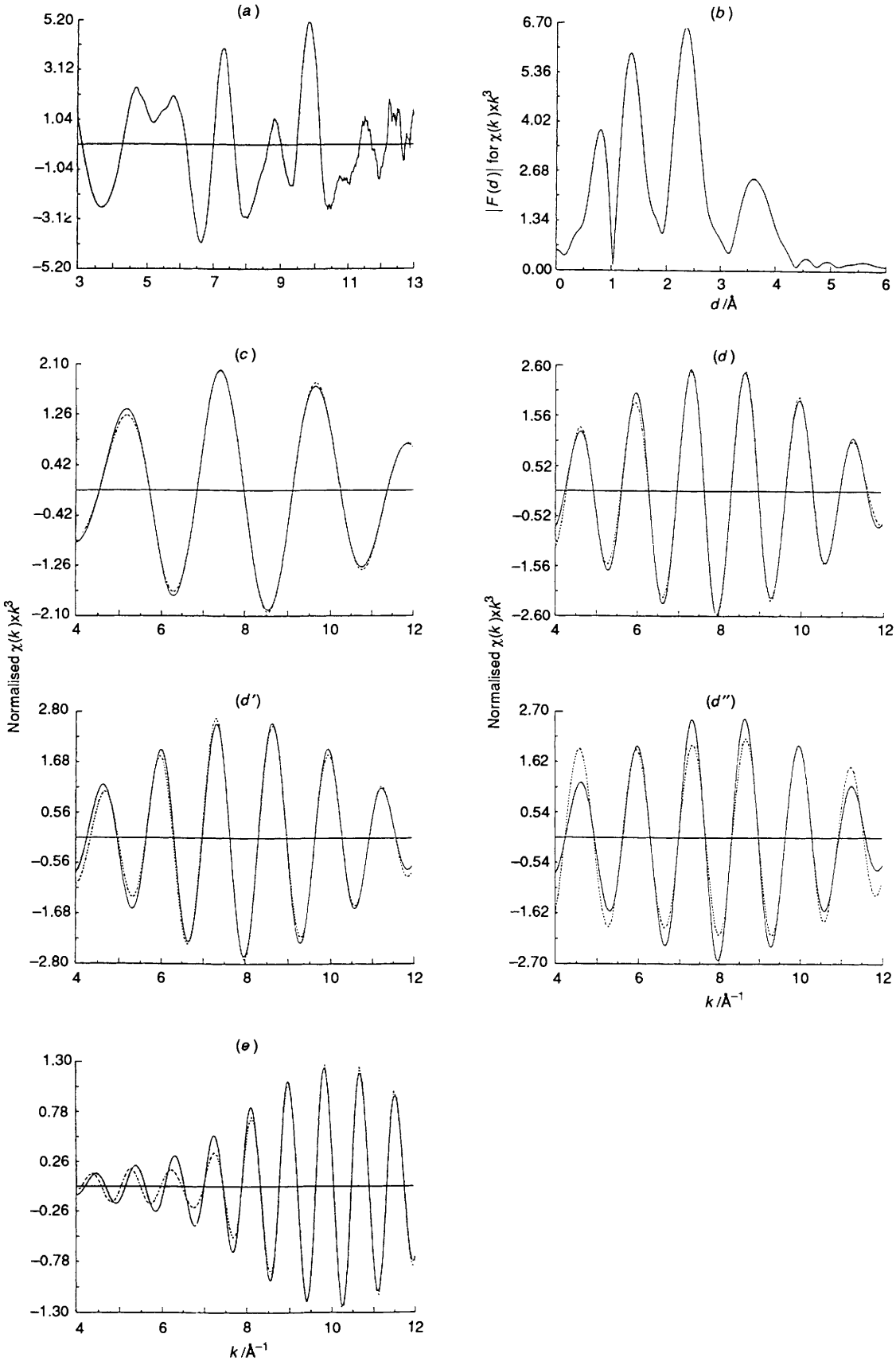

Fig. 5 The EXAFS spectra for unpretreated $[Ru_6C(CO)_{16}Me]^-$–SiO_2 at 293 K: (*a*) k^3-weighted EXAFS oscillation (smoothed), (*b*) its associated Fourier transform, and curve-fitting analyses (inversely Fourier transformed) for (*c*) Ru–C, (*d*) Ru–Ru + Ru(–C–)O [by two waves; (*d'*) and (*d"*) by one wave for Ru–Ru or for Ru(–C–)O, respectively] and (*e*) Ru(–C–)Ru (Ru–Ru second co-ordination); ——, observed; – – – –, calculated

Table 1 Curve-fitting results for the EXAFS data of $[Ru_6C(CO)_{16}Me]^-$–SiO_2 under vacuum

(*a*) Ru–C					(*b*) Ru(–C–)Ru (Ru–Ru second co-ordination)			
T/K	*N*	*d*/Å	σ/Å	*R*	*N*	*d*/Å	σ/Å	*R*
293	2.9	1.92	0.067	0.011	1.0	4.10	0.067	0.035
423	2.3	1.90	0.068	0.019	0.8	4.10	0.068	0.049
448	1.6	1.87	0.062	0.040	0.3	4.01	0.065	0.075
X-Ray[a]	2.8	1.90			1.0	4.10		

(*c*) Ru–Ru (Ru–Ru first co-ordination) + Ru(–C–)O

	Ru–Ru			Ru(–C–)O			
T/K	*N*	*d*/Å	σ/Å	*N*	*d*/Å	σ/Å	*R*
293	3.7	2.90	0.078	2.4	3.03	0.057	0.025
293	10	2.84	0.10				0.045
293				5.5	2.93	0.083	0.063
423	2.8	2.88	0.075	1.9	3.03	0.056	0.053
473[b]	4.2	2.65	0.067				0.055
X-Ray[a]	4.0	2.90		2.5	3.02		

[a] Results of X-ray analysis for $[NMe_3(CH_2Ph)][Ru_6C(CO)_{16}Me]$.[9] [b] Ru–C, Ru(–C–)O and Ru(–C–)Ru were not observed.

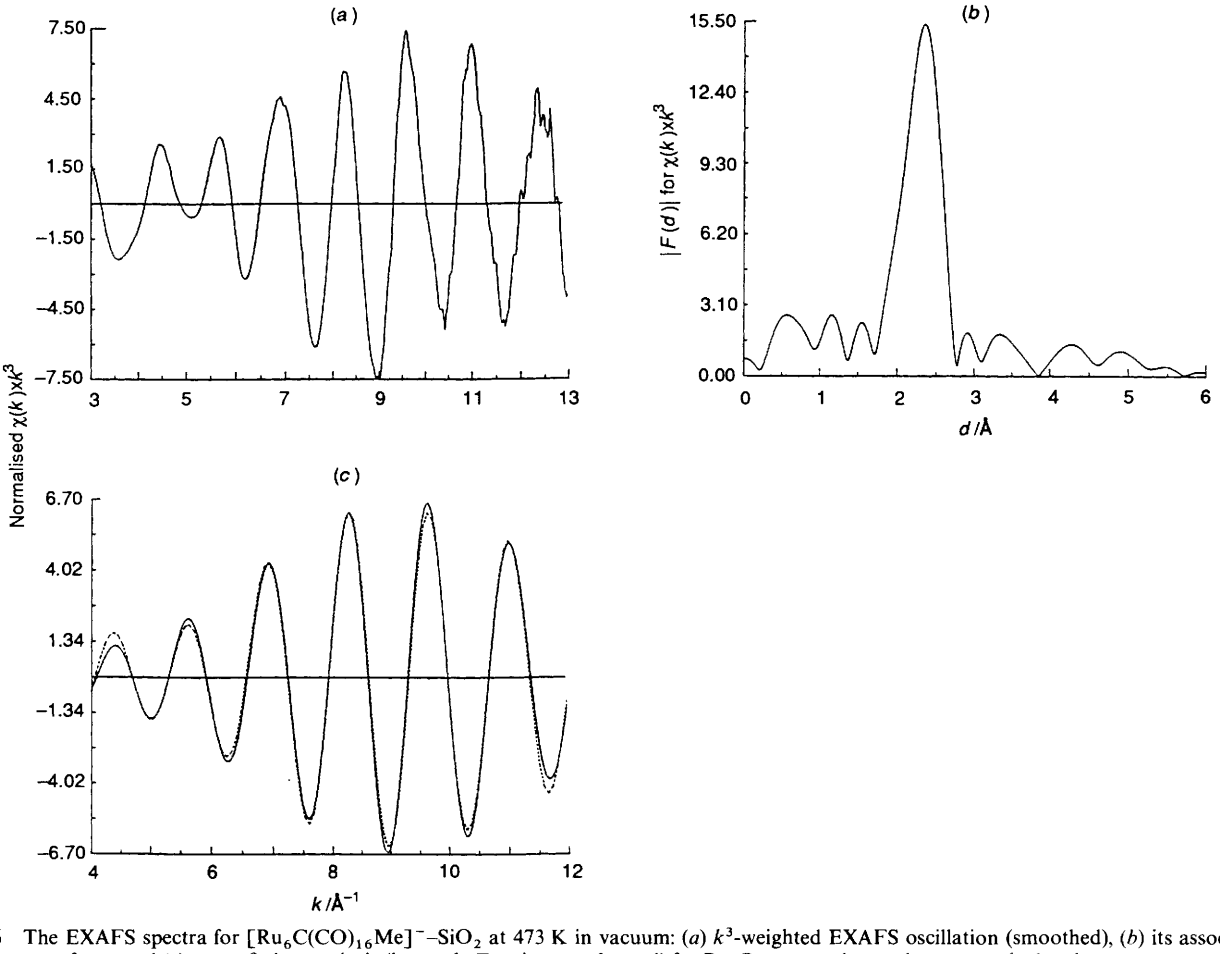

Fig. 6 The EXAFS spectra for $[Ru_6C(CO)_{16}Me]^-$–SiO_2 at 473 K in vacuum: (*a*) k^3-weighted EXAFS oscillation (smoothed), (*b*) its associated Fourier transform, and (*c*) curve-fitting analysis (inversely Fourier transformed) for Ru–Ru; ——, observed; – – – –, calculated

the similarity in distances and co-ordination numbers of the Ru–C, Ru–Ru, Ru(–C–)O and Ru(–C–)Ru bonds for both species. The structure of the supported clusters was partly decomposed at 523 K and converted into a different structure at 623 K as shown in Table 5, where only a peak due to the Ru–Ru bonds was observed.

Infrared Observation of the Interaction of $[Ru_6C(CO)_{16}Me]^-$ *with Oxide.*—Cluster **1** in CH_2Cl_2 solution exhibited the peaks in the ν_{CO} region listed in Table 6. The supported cluster, $[Ru_6C(CO)_{16}Me]^-$–SiO_2, had a similar peak pattern but the position of the main peak for terminal CO was observed at 2034s cm^{-1} compared with 2020s cm^{-1} for unsupported **1**. Fig.

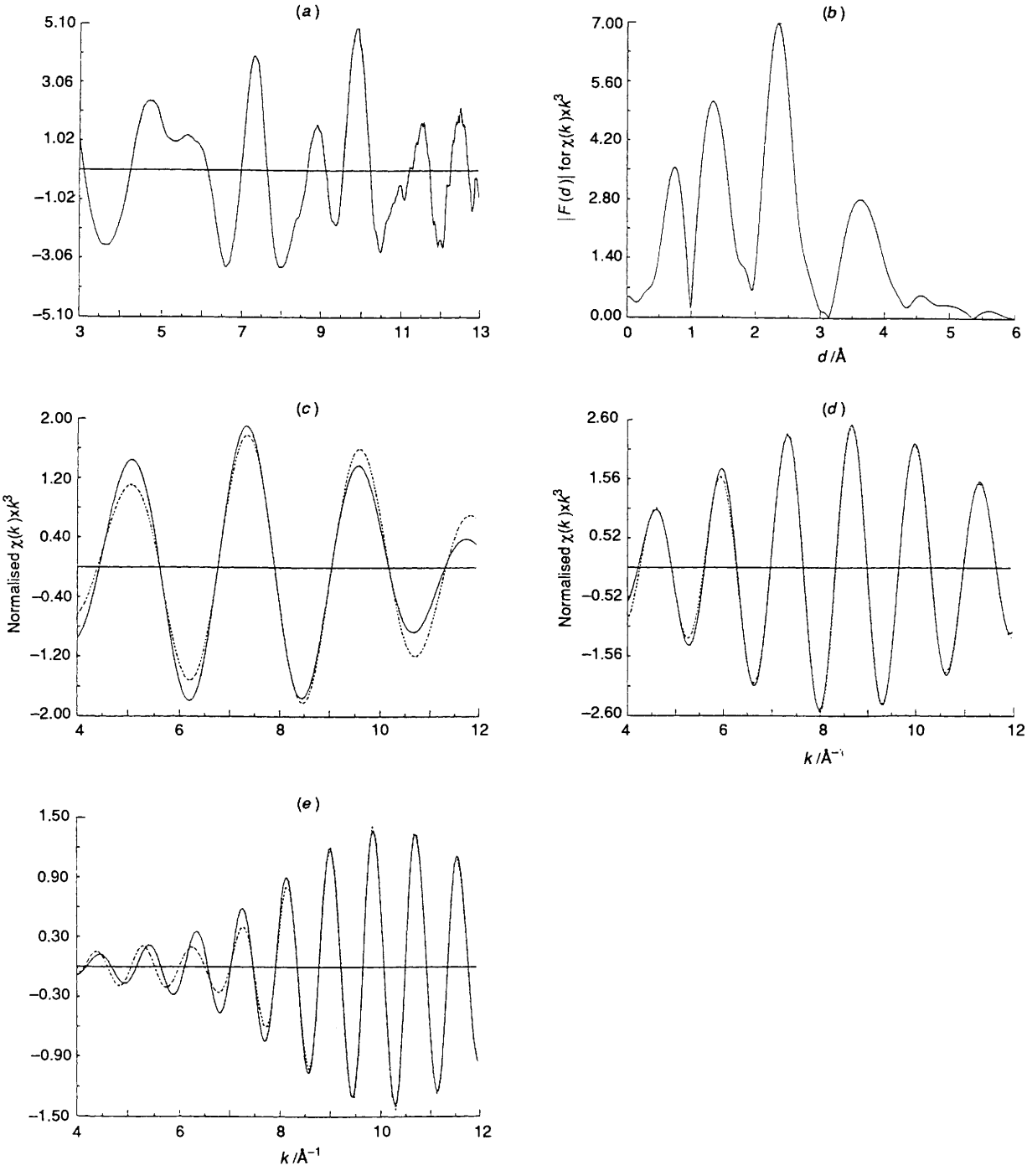

Fig. 7 The EXAFS spectra for $[Ru_6C(CO)_{16}Me]^-$–SiO_2 at 473 K under CO (13.3 kPa) + H_2 (13.3 kPa): (*a*) k^3-weighted EXAFS oscillation, (*b*) its associated Fourier transform (smoothed), and curve-fitting analyses (inversely Fourier transformed) for (*c*) Ru–C, (*d*) Ru–Ru + Ru(–C–)O and (*e*) Ru(–C–)Ru (Ru–Ru second co-ordination); ——, observed; – – – –, calculated

10 shows the IR spectra for **1** (*a*) and the supported cluster (*b*) and the peak deconvolution by Gaussians. The peaks at 1960 and 1808 cm^{-1} for **1** in Fig. 10 and Table 6 can be assigned to semi-bridging CO and bridging CO, respectively. A peak at 1986 cm^{-1} was observed for the supported cluster (1960 cm^{-1} for **1**) and its intensity became relatively larger than that for **1**.

The IR spectra in the ν_{OH} region were measured to examine the behaviour of the cluster upon supporting and heating. The relative intensity of the three ν_{OH} peaks at 3550, 3675 and 3741 cm^{-1} changed after supporting the cluster. The intensity of the peak at 3550 cm^{-1} which is assigned to hydrogen-bonded OH groups[13] decreased upon heating at 423 K under vacuum in accordance with methane formation at 373–423 K [Fig. 2(*a*)]. When the sample was heated from 323 to 473 K in CO + H_2 the intensities of the ν_{OH} peaks hardly changed. The band at 3550 cm^{-1} also decreased on heating the sample from 323 to 473 K and to 573 K under CO. For $[Ru_6C(CO)_{16}Me]^-$–Al_2O_3 and $[Ru_6C(CO)_{16}Me]^-$–TiO_2 we could not observe a definite reduction in intensity because the ν_{OH} peaks were broad or weak.

Discussion

The chemical interactions between metal clusters and oxide supports have been studied from various points of view.[14] It

Table 2 Curve-fitting results for the EXAFS data of $[Ru_6C(CO)_{16}Me]^-$–SiO_2 under CO (13.3 kPa) and H_2 (13.3 kPa)

(*a*) Ru–C					(*b*) Ru(–C–)Ru (Ru–Ru second co-ordination)			
T/K	*N*	*d*/Å	σ/Å	*R*	*N*	*d*/Å	σ/Å	*R*
293	2.8	1.91	0.065	0.024	0.9	4.11	0.068	0.035
373	2.9	1.91	0.068	0.031	0.9	4.10	0.062	0.032
423	2.7	1.92	0.052	0.034	1.0	4.11	0.065	0.040
473	2.6	1.92	0.065	0.051	1.1	4.10	0.069	0.032
X-Ray[a]	2.8	1.90			1.0	4.10		

(*c*) Ru–Ru (Ru–Ru first co-ordination) + Ru(–C–)O							
	Ru–Ru			Ru(–C–)O			
T/K	*N*	*d*/Å	σ/Å	*N*	*d*/Å	σ/Å	*R*
293	3.8	2.91	0.073	2.5	3.04	0.069	0.016
473	3.7	2.912.91	0.047	1.9	3.03	0.031	0.020
523[b]	4.5	2.66	0.066				0.049
X-Ray[a]	4.0	2.90		2.5	3.02		

Footnotes *a*, *b* as in Table 1.

Table 3 Curve-fitting results for the EXAFS data of $[Ru_6C(CO)_{16}Me]^-$–Al_2O_3 under vacuum

(*a*) Ru–C					(*b*) Ru(–C–)Ru (Ru–Ru second co-ordination)			
T/K	*N*	*d*/Å	σ/Å	*R*	*N*	*d*/Å	σ/Å	*R*
293	2.9	1.91	0.074	0.009	1.0	4.10	0.063	0.028
373	3.0	1.91	0.070	0.023	0.9	4.10	0.060	0.035
423 473	2.8 2.2	1.90	0.068	0.019	1.0	4.10	0.066	0.026
		1.89	0.073	0.072	0.3	4.10	0.066	0.070
X-Ray*	2.8	1.90			1.0	4.10		

(*c*) Ru–Ru (Ru–Ru first co-ordination) + Ru(–C–)O							
	Ru–Ru			Ru(–C–)O			
T/K	*N*	*d*/Å	σ/Å	*N*	*d*/Å	σ/Å	*R*
293	3.8	2.89	0.078	2.9	3.01	0.073	0.025
423	3.8	2.89	0.077	2.7	3.01	0.079	0.026
X-Ray*	4.0	2.90		2.5	3.02		

Ru–C, Ru(–C–)O and Ru(–C–)Ru were not observed at 673 K.

* Results of X-ray analysis for $[NMe_3(CH_2Ph)][Ru_6C(CO)_{16}Me]$.[9]

has been demonstrated that $[Ru_3(CO)_{12}]$ is physisorbed on SiO_2 and TiO_2[11] or interacts with SiO_2 and Al_2O_3 to form $[Ru_3(CO)_{10}(\mu\text{-H})(\mu\text{-OSi})]$[15,16] and $[Ru_3(CO)_{10}(\mu\text{-H})(\mu\text{-OAl})]$[11,15] by reaction with surface OH groups. These supported clusters were reported to be further converted into a monomeric $[Ru(CO)_2(OAl)_2]$ species on Al_2O_3 and a surface compound $[Ru_3(CO)_6(\mu\text{-OTi})_3]$ on TiO_2.[11] By reduction with H_2 at 723 K, the ruthenium species on V_2O_5, SiO_2, and TiO_2 were transformed into metallic clusters/particles.[11] The aggregation of clusters to species of higher nuclearity has also been reported with $[Ru_3(CO)_{12}]$ and $[Ru_4H_4(CO)_{12}]$ on SiO_2, Al_2O_3, and TiO_2.[17] The compound $[Ru_6C(CO)_{17}]$ interacts with Al_2O_3 to give $[Ru_6C(CO)_{16}]$ and one molecule of carbon monoxide.[18] The nature of the interaction of clusters with supports, the loadings of clusters, and the behaviour of supported clusters depend on the properties of the clusters and supports, and also on the atmosphere, *e.g.* in vacuum or ambient gases.

The cluster $[Ru_6(CO)_{18}]^{2-}$ is formed from $[Ru_3(CO)_{12}]$ in tetrahydrofuran (thf), and further transformed into $[Ru_6C(CO)_{16}]^{2-}$ at 435 K.[12] The latter dianion has a space for small ligands like CO and Me, and hence is methylated to stabilize the Ru_6C framework.[9] Thus, $[Ru_6C(CO)_{16}Me]^-$ is more stable than $[Ru_3(CO)_{12}]$, $[Ru_6(CO)_{18}]^{2-}$ and $[Ru_6C(CO)_{16}]^{2-}$ in homogeneous systems. Its decomposition temperature is higher than those of the other ruthenium clusters.

In the $[Ru_6C(CO)_{16}Me]^-$–SiO_2, –Al_2O_3 and –TiO_2 systems no gas evolution was observed upon supporting the anion on the oxides, suggesting physisorption at 293 K. Strong ν_{CO} peaks for $[Ru_6C(CO)_{17}]$ and $[Ru_6C(CO)_{16}Me]^-$ were observed at 2064 and 2049 and at 2020 cm^{-1}, respectively (Table 6), while the incipient $[Ru_6C(CO)_{16}Me]^-$–SiO_2 exhibited a main peak at 2034 cm^{-1}. The supported cluster may still be partially anionized on the surface. The peak at 1986 cm^{-1} was shifted to higher frequency and became relatively strong compared to the peak at 1960 cm^{-1} for the semi-bridging CO of the unsupported cluster **1**. The appearance of the band at 1986 cm^{-1} may be due to the interaction of the terminal CO with the surface upon supporting, rather than a blue shift of the band of **1** at 1960 cm^{-1}, because there are no reasons for an increase in the value for the semi-bridging CO. The band at 1808 cm^{-1} for the bridging CO groups of **1** shifted to 1768 cm^{-1} upon supporting as shown in Table 6 and Fig. 10. This red shift may be due to the interaction of the bridging CO with the surface. There are well characterized systems, $[Fe_2(\eta\text{-}C_5H_5)_2(CO)_4]$–$AlEt_3$, in which electron-rich bridging CO interacts with Lewis acids to form adducts.[19] However, the SiO_2 surface heated at 473 K is covered with OH groups rather than Lewis-acid sites. The mode

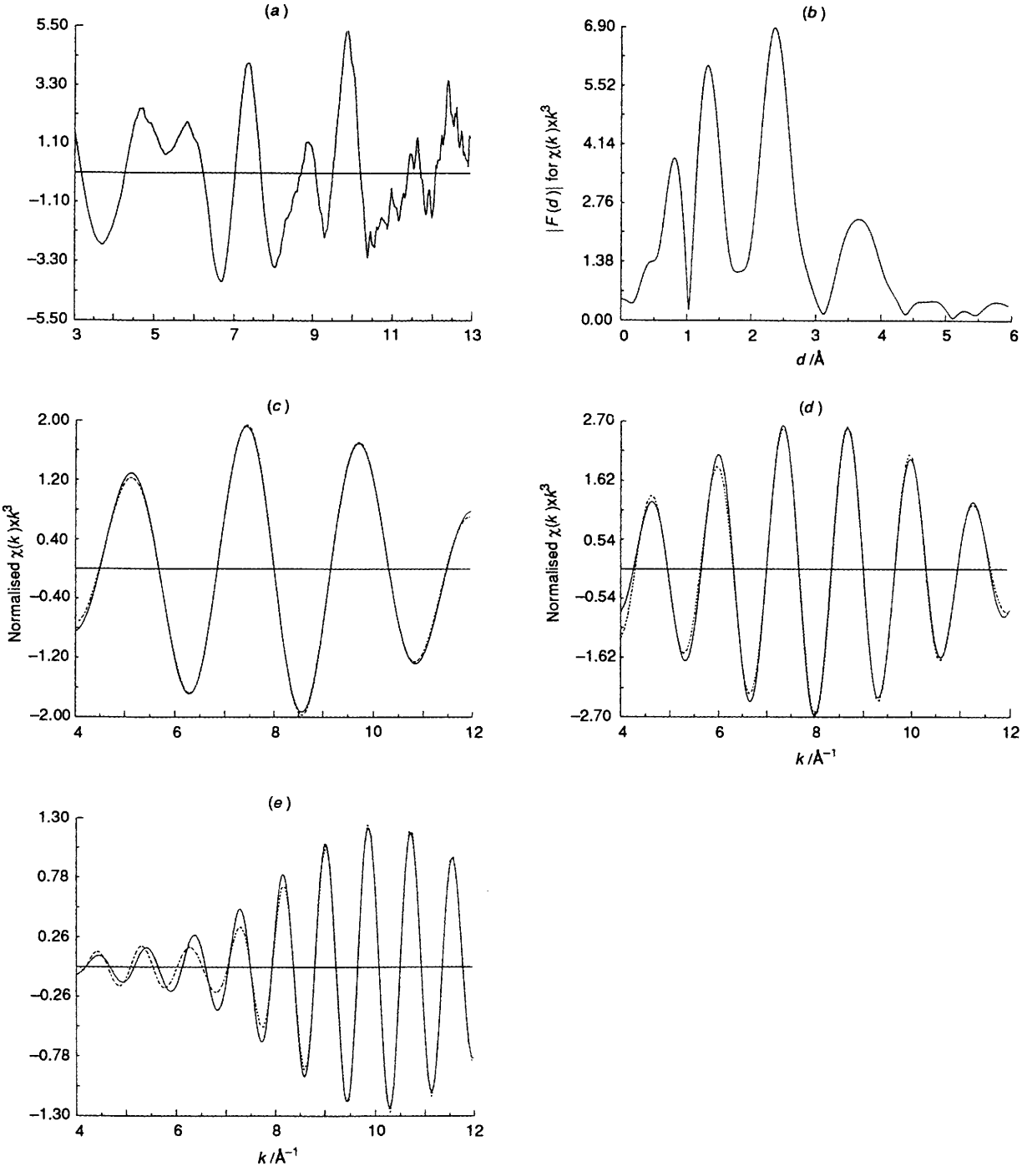

Fig. 8 The EXAFS spectra for unpretreated $[RuC(CO)_{16}Me]^-$–Al_2O_3 at 293 K: (*a*) k^3-weighted EXAFS oscillation (smoothed), (*b*) its associated Fourier transform, and curve-fitting analyses (inversely Fourier transformed) for (*c*) Ru–C, (*d*) Ru–Ru + Ru(–C–)O and (*e*) Ru(–C–)Ru (Ru–Ru second co-ordination); ——, observed; – – – –, calculated

of the interaction may be different between the two systems. Thus, the $[Ru_6C(CO)_{16}Me]^-$ cluster is suggested to be physisorbed with the bridging and terminal CO on the SiO_2 surface. An IR examination of the phenyl-framework stretching shows that the counter cation $[NMe_3(CH_2Ph)]^+$ remains on SiO_2 up to *ca.* 623 K.

The EXAFS Fourier transforms and the curve-fitting analyses for the Ru–Ru second co-ordination peak [Ru(–C–)Ru] in Figs. 5–9 and Tables 1–5 showed that the cluster structure was retained on SiO_2, Al_2O_3 and TiO_2 at 293 K, no ligands being desorbed according to the gas-phase analysis. The thermal stability of the cluster framework varied depending on the kinds of oxide and ambient gas. The Ru–Ru peak for the linear Ru–C–Ru conformation is generally relatively more intense compared with that for the bent structure or no-carbon Ru–Ru bond at similar bond length (second or third co-ordination). The co-ordination number of the Ru(–C–)Ru bond can be used as an indicator of the retention of the Ru_6C framework. In vacuum $[Ru_6C(CO)_{16}Me]^-$–SiO_2, –Al_2O_3 and –TiO_2 were stable until 423 K as shown in Tables 1 and 3. In the presence of CO (13.3 kPa) + H_2 (13.3 kPa) the clusters supported on SiO_2 and TiO_2 were stable until 473 K as shown in Tables 2 and 5, and that on Al_2O_3 was even stable at 523 K (Table 4).

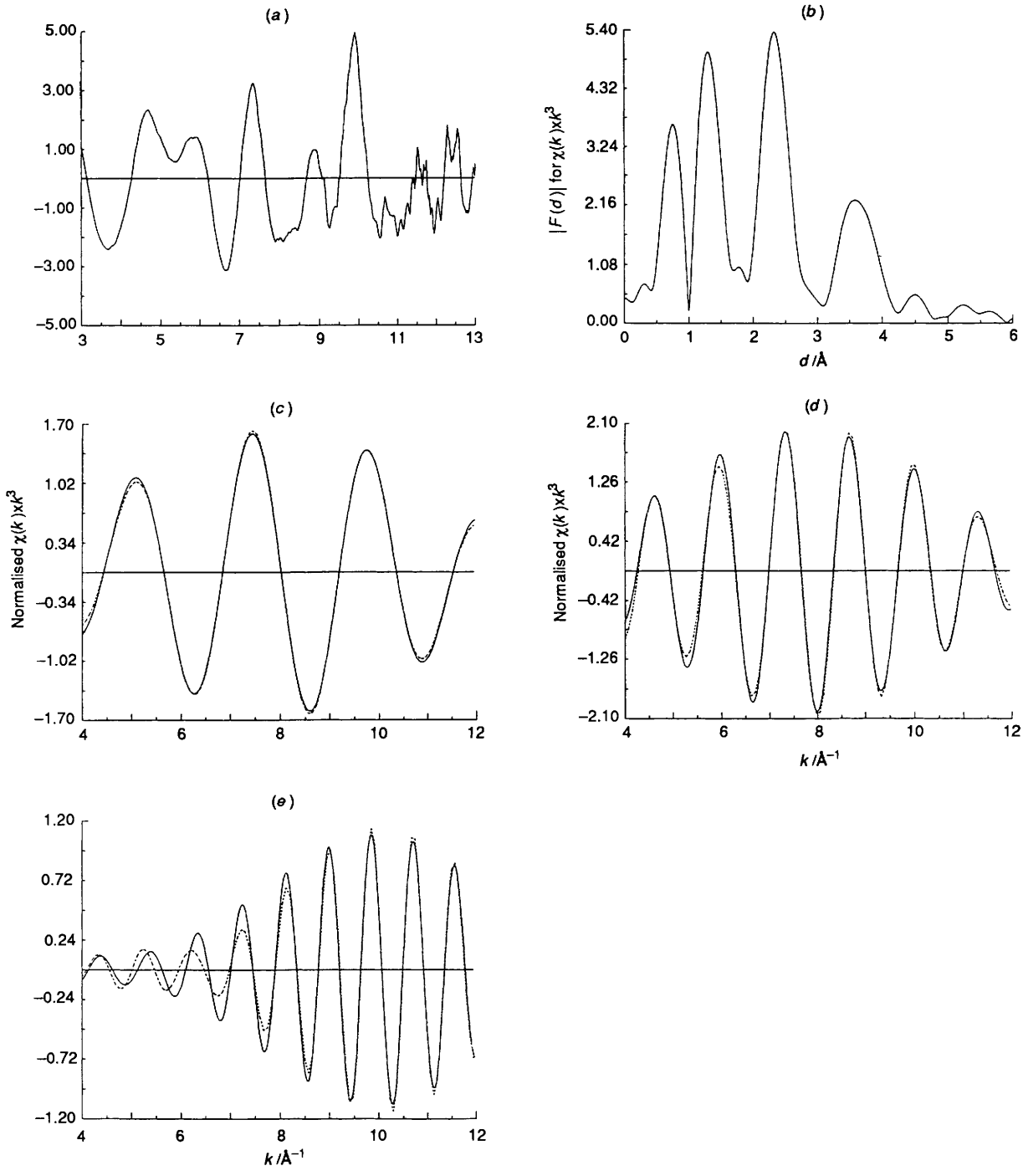

Fig. 9 The EXAFS spectra for $[Ru_6C(CO)_{16}Me]^-$–Al_2O_3 at 523 K under CO (13.3 kPa) + H_2 (13.3 kPa): (*a*) k^3-weighted EXAFS oscillation (smoothed), (*b*) its associated Fourier transform, and curve-fitting analyses (inversely Fourier transformed) for (*c*) Ru–C, (*d*) Ru–Ru + Ru(–C–)O and (*e*) Ru(–C–)Ru (Ru–Ru second co-ordination); ——, observed; – – – –, calculated

The formation of acetaldehyde *via* insertion of CO into the methyl ligand was observed in the TPD spectra for the supported clusters under CO and/or H_2. In vacuum all the methyl ligands reacted with surface OH groups at 373–473 K. The reactive OH groups are suggested to be mainly of hydrogen-bonded type, according to the IR spectra. The TPD spectra in H_2 showed the formation of acetaldehyde with the selectivities of 43 and 8% for the SiO_2 and Al_2O_3 systems, respectively. This means that the acetyl species were hydrogenated by gas-phase H_2 rather than the surface OH. Acetaldehyde was also observed from the TPD spectra under CO as shown in Fig. 2(*c*) (23 and 3% for SiO_2 and Al_2O_3). Gas-phase CO stabilizes the Ru_6C framework as demonstrated by EXAFS and may retard the conversion of acetyl back into methyl and carbonyl ligands. In this context acetaldehyde formation may be favoured by the stabilization effect of CO and the hydrogenation of acetyl by H_2. The high selectivity to acetaldehyde was found in Figs. 2(*d*), 3(*b*) and 4 (77, 15 and 10% for SiO_2-, Al_2O_3- and TiO_2-supported clusters, respectively). The maximum acetaldehyde formation for the SiO_2-supported cluster occurred at 443 K which is lower than the decomposition temperature of the Ru_6C framework. On the contrary the TPD peak for acetaldehyde was observed at 543 K on Al_2O_3 which is near the decomposition temperature as shown by EXAFS. This structural difference between

Table 4 Curve-fitting results for the EXAFS data of $[Ru_6C(CO)_{16}Me]^-$–Al_2O_3 under CO (13.3 kPa) and H_2 (13.3 kPa)

(*a*) Ru–C

T/K	*N*	*d*/Å	σ/Å	*R*
293	3.0	1.91	0.075	0.010
373	3.0	1.91	0.063	0.012
473 523	2.9	1.91	0.069	0.020
	2.6	1.89	0.070	0.009
X-Ray[a]	2.8	1.90		

(*b*) Ru(–C–)Ru (Ru–Ru second co-ordination)

N	*d*/Å	σ/Å	*R*
1.0	4.11	0.063	0.031
1.0	4.10	0.065	0.019
1.1	4.10	0.062	0.038
1.0	4.09	0.063	0.041
1.0	4.10		

(*c*) Ru–Ru (Ru–Ru first co-ordination) + Ru(–C–)O

	Ru–Ru			Ru(–C–)O			
T/K	*N*	*d*/Å	σ/Å	*N*	*d*/Å	σ/Å	*R*
293	3.9	2.89	0.072	2.6	3.03	0.073	0.020
473	3.9	2.89	0.070	2.4	3.02	0.075	0.022
523	3.8	2.88	0.078	2.5	3.01	0.073	0.025
573[b]	4.2	2.68	0.063				0.041
X-Ray[a]	4.0	2.90		2.5	3.02		

Footnotes *a*, *b* as in Table 1.

Table 5 Curve-fitting results for the EXAFS data of $[Ru_6C(CO)_{16}Me]^-$–TiO_2 in CO (13.3 kPa) and H_2 (13.3 kPa)

(*a*) Ru–C

T/K	*N*	*d*/Å	σ/Å	*R*
293	2.9	1.92	0.060	0.034
373	2.9	1.92	0.065	0.019
473 523	2.4	1.91	0.065	0.027
	1.6	1.87	0.061	0.035
X-Ray[a]	2.8	1.90		

(*b*) Ru(–C–)Ru (Ru–Ru second co-ordination)

N	*d*/Å	σ/Å	*R*
0.9	4.10	0.049	0.032
0.9	4.09	0.060	0.028
0.9	4.10	0.047	0.020
0.3	4.10	0.062	0.080
1.0	4.10		

(*c*) Ru–Ru (Ru–Ru first co-ordination) + Ru(–C–)O

	Ru–Ru			Ru(–C–)O			
T/K	*N*	*d*/Å	σ/Å	*N*	*d*/Å	σ/Å	*R*
293	4.0	2.90	0.070	2.0	3.02	0.043	0.022
373	3.9	2.90	0.070	2.0	3.02	0.058	0.022
473	3.9	2.89	0.075	2.0	3.02	0.049	0.023
623[b]	3.3	2.63	0.075				0.052
X-Ray[a]	4.0	2.90		2.5	3.02		

Footnotes *a*, *b* as in Table 1.

Table 6 Infrared bands (cm^{-1}) for $[NMe_3(CH_2Ph)][Ru_6C(CO)_{16}Me]$, $[Ru_6C(CO)_{16}Me]^-$–SiO_2 and related clusters

Cluster	Bands	Ref.
$[Ru_6C(CO)_{16}Me]^-$	2074w, 2020s, 1960m, 1808m (br)	This work
$[Ru_6C(CO)_{16}Me]^-$–SiO_2		
295 K	2074w, 2034s, 1986m, 1768m (br)	This work
473 K *	2070w, 2045 (sh), 2031m, 1988s, 1769m (br)	This work
$[Ru_6C(CO)_{16}]^{2-}$	2048w, 2032w, 1977s, 1952m (sh), 1918m, 1820m (sh), 1780m	12
$[Ru_6C(CO)_{17}]$	2064s, 2049s, 2007w, 1993w, 1958w, 1854w (br)	12
$[Ru_6C(CO)_{16}(COMe)]^-$	2067w, 2013s, 1966w, 1805m (br), 1662w (br)	9

* In CO + H_2.

the clusters supported on SiO_2 and Al_2O_3 may be related to the difference in the selectivity of acetaldehyde formation on SiO_2 (77%) and Al_2O_3 (15%). The supported system $[Ru_6C(CO)_{16}Me]^-$–SiO_2 showed a higher selectivity than its thermally decomposed microparticle species for ethene hydroformylation.[20] The lower selectivity observed with the TiO_2-supported cluster cannot easily be explained, but the concentration of acetyl at the hydrogenation temperature might be low. It is to be noted that MeOH was produced during the TPD in CO and CO + H_2 for the Al_2O_3- and TiO_2-supported clusters in Figs. 2(*d*), 3(*b*) and 4, indicating the possibility of the development of new catalytic systems which produce alcohols from CO/H_2 unlike the usual ruthenium particles.

The $[Ru_6C(CO)_{16}Me]^-$ clusters supported on SiO_2 and Al_2O_3 were decomposed to ruthenium at 448 and 473 K, respectively, under vacuum. The decomposition temperatures of the SiO_2-, Al_2O_3- and TiO_2-supported clusters under CO or CO + H_2 increased to 523, 573 and 523 K, respectively. The

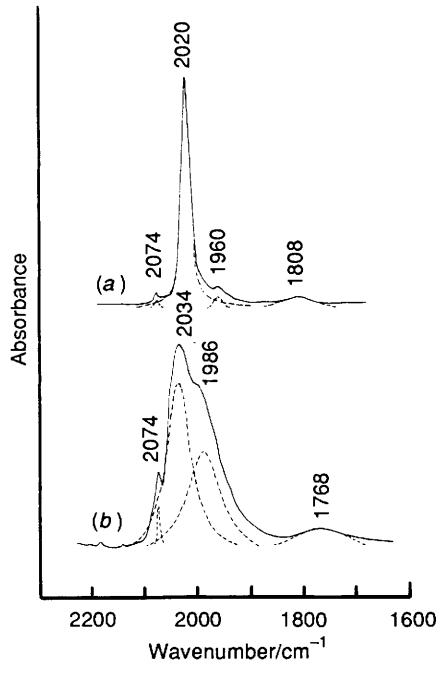

Fig. 10 Peak deconvolutions of IR spectra for $[NMe_3(CH_2Ph)][Ru_6C(CO)_{16}Me]$ (*a*) and untreated $[Ru_6C(CO)_{16}Me]^-$–SiO_2 (*b*)

obtained ruthenium samples showed similar co-ordination numbers for the Ru–Ru bond to those for the incipient supported clusters as shown in Tables 1, 2, 4 and 5, which suggest the retention of the Ru_6 unit on these surfaces at 523–573 K.

Uchiyama and Gates[21] observed that the stable cluster $[Ru_6C(CO)_{16}]^{n-}$ was formed from $[Ru_3(CO)_{12}]$, $[Ru_4H_4(CO)_{12}]$ and $RuCl_3 \cdot xH_2O$ on MgO under CO/H_2 reaction conditions (548 K, 1.0–7.1 MPa, CO/H_2 = 1:1).[21] However, they reported that this cluster on MgO was inactive for CO/H_2 reaction. In contrast, the $[Ru_6C(CO)_{16}Me]^-$–SiO_2 catalyst showed a higher selectivity than a conventional Ru/SiO_2 catalyst for catalytic ethene hydroformylation. During the reaction the Ru_6C cluster framework was suggested to be maintained.[20]

Conclusion

The salt $[NMe_3(CH_2Ph)][Ru_6C(CO)_{16}Me]$ has been used as a precursor to obtain stable clusters on oxide surfaces and to examine the role of the cluster framework (metal–metal bond) in insertion of CO and catalytic hydroformylation. The structures of the clusters supported on SiO_2, Al_2O_3 and TiO_2 were characterized by EXAFS [Ru–C, Ru–Ru, Ru(–C–)O and Ru(–C–)Ru bonds] and TPD. The cluster was physisorbed *via* the interaction of the bridging and terminal CO groups with the oxides at 293 K, and at 373–473 K in vacuum reacted with mainly hydrogen-bonded OH groups of the oxide surfaces to form methane. Under vacuum the supported clusters were decomposed to different species with small Ru–Ru co-ordination numbers at 448–473 K, releasing ligands, whereas under CO or CO + H_2 the supported clusters were stable at those temperatures. Acetaldehyde was selectively produced in the TPD spectra under CO + H_2 in contrast to methane formation in a homogeneous system: the selectivity was 77 (SiO_2), 15 (Al_2O_3) and 10% (TiO_2).

References

1 F. Carderazzo, *Angew. Chem., Int. Ed. Engl.*, 1977, **16**, 299.
2 M. Pańkowsky and M. Bigorgne, *J. Organomet. Chem.*, 1983, **251**, 333.
3 S. C. Wright and M. C. Baird, *J. Am. Chem. Soc.*, 1985, **107**, 6899.
4 A. Dedieu, S. Sakaki, A. Strich and P. E. M. Siegbahn, *Chem. Phys. Lett.*, 1987, **133**, 317.
5 N. Koga and K. Morokuma, *J. Am. Chem. Soc.*, 1985, **107**, 7230.
6 G. Pacchioni, P. Fantucci, J. Koutecký and V. Ponec, *J. Catal.*, 1988, **112**, 34.
7 Y. Izumi, K. Asakura and Y. Iwasawa, *J. Catal.*, 1991, **127**, 631.
8 Y. Izumi, K. Asakura and Y. Iwasawa, *J. Catal.*, 1991, **132**, 566.
9 T. Chihara, K. Aoki and H. Yamazaki, *J. Organomet. Chem.*, 1990, **383**, 367.
10 T. Chihara and H. Yamazaki, unpublished work.
11 K. Asakura, K. Bando and Y. Iwasawa, *J. Chem. Soc., Faraday Trans.*, 1990, 2645; K. Asakura and Y. Iwasawa, *J. Chem. Soc., Faraday Trans.*, 1990, **86**, 2657.
12 C. Hayward and J. R. Sharpley, *Inorg. Chem.*, 1982, **21**, 381; C. R. Eady, P. F. Jackson, B. F. G. Johnson, J. Lewis, M. C. Malatesta, M. McPartlin and W. J. H. Nelson, *J. Chem. Soc., Dalton Trans.*, 1980, 383.
13 Y. Iwasawa (Editor), *Taylored Metal Catalysts*, Reidel, Dordrecht, 1986.
14 B. C. Gates, L. Guczi and H. Knözinger (Editors), *Metal Cluster in Catalysis*, Elsevier, Amsterdam, 1986.
15 J. Evans and G. S. McNulty, *J. Chem. Soc., Dalton Trans.*, 1984, 1123.
16 N. Binsted, J. Evans, G. N. Greaves and R. J. Price, *Organometallics*, 1989, **8**, 613.
17 D. J. Hunt, R. B. Moyes, P. B. Wells, S. D. Jackson and R. Whyman, *J. Chem. Soc., Faraday Trans. 1*, 1986, 189.
18 V. L. Kuznetsov, A. Bell and Y. I. Yermakov, *J. Catal.*, 1980, **65**, 374.
19 N. E. Kim, N. J. Nelson and D. F. Shriver, *Inorg. Chim. Acta*, 1973, **7**, 393.
20 Y. Izumi, T. Chihara, H. Yamazaki and Y. Iwasawa, unpublished work.
21 S. Uchiyama and B. C. Gates, *J. Catal.*, 1988, **110**, 388.

Received 6th March 1992; *Paper* 2/01229D